TECTONIC-STRESS MAP ACROSS ENCELADUS' SPT AND POSSIBLE MECHANICAL CAUSES

A. M. Schoenfeld[1] and A. Yin[1]
[1]Department of Earth, Planetary, and Space Sciences and the Institute of Planets and Exoplanets, University of California, Los Angeles, CA 90095-1567, USA

Introduction: The outer solar system consists of a diverse population of icy satellites, but our understanding of their evolution remains in its infancy. Enceladus, a small (diameter ~500 km) moon of Saturn, provides a unique opportunity to explore the mechanical behaviors of icy satellites due to its unique geology, characterized by cyclically erupting geysers at the moon's south pole. The plumes of these geysers are sourced from a series of parallel ''tiger-stripe" fractures (TSF), and are composed of gas and water-ice particulate. Plume materials originate from a global water ocean beneath Enceladus' outer ice shell, making Enceladus a leading candidate in the search for extraterrestrial life [1].

The cyclic nature of the plume's eruption, the periodicity of which matches the orbital period of the satellite, has been attributed to daily variations of tidal stresses acting on the moon [2]. These daily stresses are thought to be a consequence of Enceladus' eccentric orbit around Saturn. However, there is an offset in timing between Cassini's observations of peak eruption and what is predicted by the theory of tidally modulated cracks as driven by orbital eccentricity [3].

Existing models have attempted to reconcile the plume timing discrepancy by invoking stress relaxation in a viscoelastic ice sell [3][4][5]. However, such an approach assumes the stress in the ice shell to be entirely induced by tidal stress, neglecting the role tectonically induced stress play in order to support the high (>1 km) topographic relief around the moon's south pole [6]. We propose to relax the assumption of a tectonic stress-free ice shell and first offer an analytical tensor analysis decomposing tidal and tectonic stresses. Then, we introduce two semi-qualitative stress field calculation in order to begin exploring the origin of the tectonic stresses we derive from the aforementioned decomposition model.

Methodology: We investigate the total stress as a result of three stress sources: tidal stress creating an averaged bulge figure, stress induced by physical libration, and tectonic stresses. We hypothesize that the observed delay in eruption is a result of the relative difference in magnitude of these three stresses. The mathematical framework we employ to calculate tidal stress follows the expression for varying stress as described by the Vening-Meinesz equations [4] for a decoupled, thin shell. The total stress can be represented as:

$$\sigma_{ij}^{SUM}(x,y,t) = \sigma_{ij}^{L}(x,y,t) + \sigma_{ij}^{B}(x,y) + \sigma_{ij}^{T}(x,y)$$

where σ_{ij}^{SUM} is the total stress tensor, σ_{ij}^{L} is the libration-induced stress tensor, σ_{ij}^{B} is the tidal bulge-induced stress tensor, and σ_{ij}^{T} is the tectonic stress tensor.

We are interested in deriving the tectonic stresses at the South Polar Terrain (SPT) for when the tiger-stripe fractures are at the state of frictional instability. Thus, we assume the fault is at the critical stress of tensile failure (plume eruption), such that $\sigma_1^D = \rho g h/2$ and $\sigma_3^D = -T_0$, where T_0 is tensile strength of the brittle ice shell, ρ is the ice-shell density, and g is gravity on the surface. Our goal is to determine the magnitude of σ_3^T and thus the tectonic stress tensor. This can be achieved by solving first for the tensor components of $\sigma_{ij}^{SUM}(x, y)$, and then for the tensor components of $\sigma_{ij}^{T}(x, y)$. We use this analytical approach to deduce the magnitude and direction of tectonic stress tensors at points corresponding to active jets as observed by Cassini [7].

Results: We calculated the maximum shear stresses for an ice shell 10 km thick and with a tensile strength of $T_0 = 10^6$ Pa, $5\text{x}10^6$ Pa, and 10^7 Pa. We do this for the point in the orbit 5 hours past periapsis (peak eruption). The preliminary results for maximum shear are plotted on an ISS mosaic of Enceladus' SPT in Figure 1. The results indicate that the magnitude of maximum shear varies systematically across the TSF: it appears generally higher on the sub-saturnian face of the mosaic, and generally lower moving towards the anti-saturnian face. There is also local variability at fault branching points. The largest concentration of large maximum shear values are found adjacent to regions of compressional faulting along the subsaturnian (SSM)/trailing edge margin (TEM) (Figure 2).

The preliminary results for orientation of σ_1^T are also plotted in Figure 1 (black lines). Results indicate a general trend of sinusoidal rotation across the TSF, the orientation of σ_1^T oscillating across the SPT, trending from the LEM to the TEM. Results once more indicate local variability within fault branches. The overall trend of these results suggests toroidal motion, and are consistent with regional clockwise rotation across the SPT and left-slip bookshelf faulting along the TSFs [8].

Possible Mechanical Causes: We begin to explore the possible mechanical origin of these inferred tectonic stresses by introducing two semi-qualitative stress field calculations. First, we calculate the stress field at the SPT due to gravitational spreading from uneven ice shell thickness [8][9] plus rotation of the SPT that would accommodate bookshelf faulting of the TSF [8].

Then, we calculate the stress field due to basal sliding along the brittle-ductile transition zone (similar to detachment faults of earth) [9][10] plus rotational shear [8]. The results are presented in Figure 2. We find that the stress field for gravitational spreading plus rotation fits our derived tectonic values the best, both in range of magnitudes and in distribution of stresses. However, both models fail to predict the dramatically lower tectonic magnitudes (~10^2–10^3 Pa) sporadically found along the TSF, which is likely is indicative of a more complex stress field. Explaining the derived tectonic stresses of Figure 1 is a non-unique problem, thus further mechanical scenarios and combinations need to be explored in future work.

Limitations: This work is just the first step in a greater exploration of ice-shell deformation and tectonics. We do not evaluate how stress interacts spatially within this simple analytical framework; we are only evaluating singular points along the fault, without insight into how their locations are kinematically linked. In addition, we assume only that the shell has tensile strength, and for simplification purposes do not include rheological constraints. We likewise present two simple, semi-qualitative results calculating the stress field for two different mechanical origins in an effort to begin exploring the origin of the tectonic stresses shown in Figure 1. In our calculations, we regard the SPT as a two dimensional disk, and do not consider curvature.

Future Work: Eventually, we intend to build a numerical model with visco-elasto-plastic rheology in order to explore ice-shell deformation processes at various time scales; these tectonic calculations will offer a quantitative constraint for that model. There are three end-member geologic scenarios we are interested in exploring with these contraints: gravitational spreading [11], basal shearing [8][10], localized plume upwelling [12], and nonsynchronous rotation [13]. Tidal stressing no doubt drives short-term plume activities at the pole, yet we propose that non-tidal, endogenic conditions are perhaps primarily responsible for the observed delay in plume eruption.

References: [1] Porco et al. (2006) *Science, 311*, 1393-1401. [2] Hurford et al. (2007) *Nature, 447*, 292-294. [3] Nimmo et al. (2014) *The Astronomical Journal, 148*, 46-60. [4] Hurtford et al. (2009) *Icarus, 203*, 541-552. [5] Běhounková et al. (2015), *Nature, 8*, 601-606. [6] Schenk and McKinnon (2009) *Geophysical Research Letters, 36*, L16202. [7] Porco et al. (2014) *The Astronomical Journal, 148*. [8] Yin and Pappalardo (2015), *Icarus, 260*, 409-439. [9] Yin et al. (2016), *Icarus, 266*, 204-216. [10] Yin (1989), *Tectonics, 8*, 469-482. [11] Nimmo and Manga (2010), *Univ. of Arizona Press*, 381- 404. [12] Showman and Barr (2009) *Univ. Arizona Press*, 405-430. [13] Patthoff and Kattenhorn (2011), *Geophysical Research Letters, 38*, L18201.

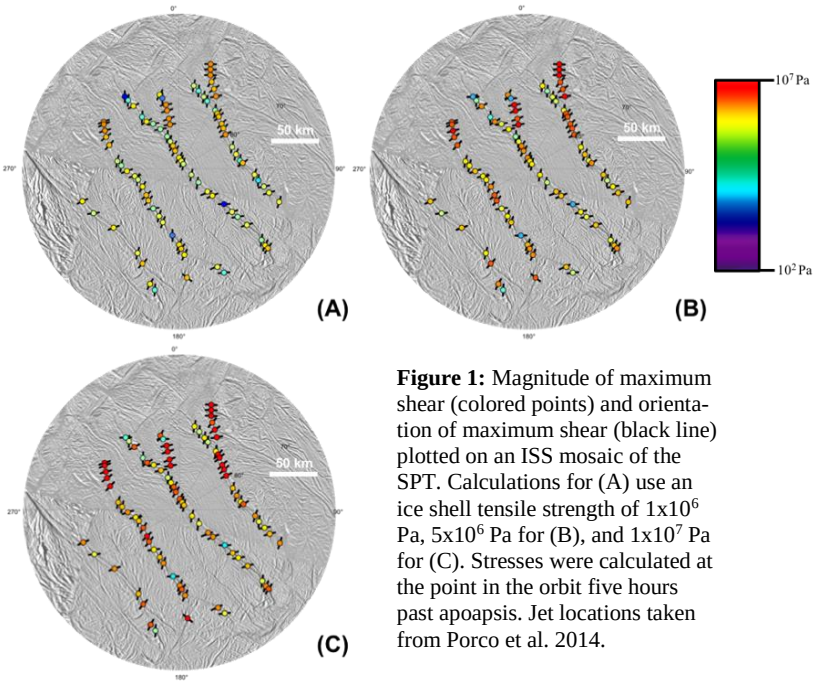

Figure 1: Magnitude of maximum shear (colored points) and orientation of maximum shear (black line) plotted on an ISS mosaic of the SPT. Calculations for (A) use an ice shell tensile strength of $1x10^6$ Pa, $5x10^6$ Pa for (B), and $1x10^7$ Pa for (C). Stresses were calculated at the point in the orbit five hours past apoapsis. Jet locations taken from Porco et al. 2014.

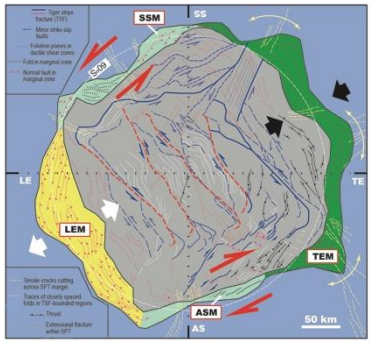

Figure 2: Interpreted structural map of the SPT from Yin and Pappalardo (2015). SSM stands for the "sub-saturnian margin", TEM stands for the "trailing-Edge Margin", ASM stands for the "anti-saturnian margin", and LEM stands for the "leading-edge margin". The LEM corresponds to a region of compressional faulting, while the TEM corresponds to a region of extensional faulting.

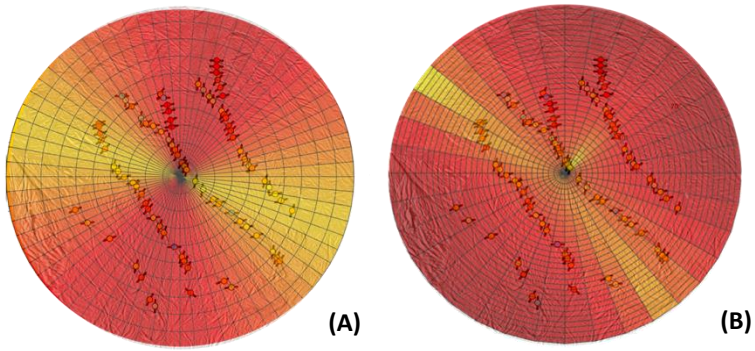

Figure 3: We explore various mechanical processes in order to match the tectonic stresses derived from our decomposition mode. (A) The resultant maximum shear stress field generated by superposing gravitational spreading and rotational shear. (B) The resultant maximum shear stress field generated by superposing basal shear and rotational shear. Both are overlain over plot B from figure 1 ($T_0 = 5x10^6$ Pa). The color scheme here corresponds to the color bar from figure 1.